JCIM JOURNAL OF CHEMICAL INFORMATION AND MODELING

Article

pubs.acs.org/jcim

Combined Experimental and Molecular Simulation Study of Insulin–Chitosan Complexation Driven by Electrostatic Interactions

Cecilia Prudkin-Silva,[†] Oscar E. Pérez,[†] Karina D. Martínez,[‡] and Fernando L. Barroso da Silva*[,§,∥]

[†]Departamento de Química Biológica, Facultad de Ciencias Exactas y Naturales, Instituto de Química Biológica de la Facultad de Ciencias Exactas y Naturales, IQUIBICEN-CONICET, Universidad de Buenos Aires, Buenos Aires, Intendente Güiraldes, s/n, Ciudad Universitaria, Pabellón 2, Buenos Aires CP 1428, Argentina

[‡]Departamento de Industrias, Facultad de Ciencias Exactas y Naturales, Consejo Nacional de Investigación Científica y Técnicas de la República Argentina, ITAPROQ-CONICET, Universidad de Buenos Aires, Intendente Güiraldes, s/n, Ciudad Universitaria, Buenos Aires CP 1428, Argentina

[§]Departamento de Física e Química, Faculdade de Ciências Farmacêuticas de Ribeirão Preto, Universidade de São Paulo, Ribeirão Preto, São Paulo, 05508-220 Brazil

[∥]Department of Chemical and Biomolecular Engineering, North Carolina State University, Raleigh, North Carolina 27695, United States

Supporting Information

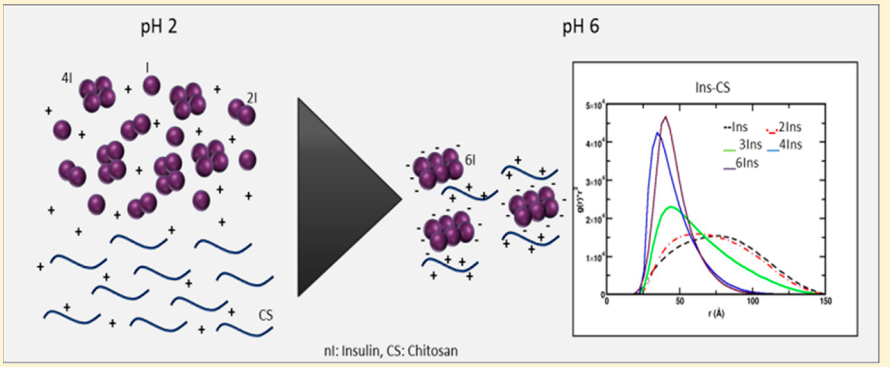

ABSTRACT: Protein–polysaccharide complexes constructed via self-assembly methods are often used to develop novel biomaterials for a wide range of applications in biomedicine, food, and biotechnology. The objective of this work was to investigate theoretically and to demonstrate via constant-pH Monte Carlo simulations that the complexation phenomenon between insulin (INS) and the cationic polyelectrolyte chitosan (CS) is mainly driven by an electrostatic mechanism. Experimental results obtained from FTIR spectra and ζ-potential determinations allowed us to complement the conclusions. The characteristic absorption bands for the complexes could be assigned to a combination of signals from CS amide I and INS amide II. The second peak corresponds to the interaction between the polymer and the protein at the level of amide II. INS–CS complexation processes not expected when INS is in its monomeric form, but for both tetrameric and hexameric forms, incipient complexation due to charge regulation mechanism took place at pH 5. The complexation range was observed to be 5.5 < pH < 6.5. In general, when the number of INS units increases in the simulation process, the solution pH at which the complexation can occur shifts toward acidic conditions. CS's chain interacts more efficiently, i.e. in a wider pH range, with INS aggregates formed by the highest monomer number. The charge regulation mechanism can be considered as a previous phase toward complexation (incipient complexation) caused by weak interactions of a Coulombic nature.

1. INTRODUCTION

Over the last years, much attention has been focused on pH-responsive macromolecular mechanisms involved in protein–polysaccharide interactions, as a tool for designing novel structures with new functionalities.[1] Thus, protein–polysaccharide complexes constructed via self-assembly method were often used as building blocks, to develop novel biomaterials for a wide range of applications in biomedicine, food, and biotechnology.[2,3] Self-assembly is a ubiquitous and natural process that lead to complex nanostructures with outstanding functionalities.[4] In particular, the implementation of pH-

Special Issue: Molecular Simulation in Latin America: Coming of Age

Received: September 19, 2019
Published: December 2, 2019

DOI: 10.1021/acs.jcim.9b00814
J. Chem. Inf. Model. XXXX, XXX, XXX–XXX

dependent responsive mechanisms was proven to be useful for fabrication of pharmaceutical products resembling natural protein assemblies.[5]

Several types of proteins and polysaccharides have been used for complexation. For example, Palao-Suay and collaborators describe the use of self-assembling polysaccharides such as dextran, chitosan, heparin, and alginate conjugated with anticancer drugs such as doxorubicin, camptothecin, and methotrexate.[6] In regard to the food industry, it is a common treatment to use proteins to ensure metabolic regulations for beverage/solid applications, such as the soluble whey protein−pectin complex as examined by Wagoner and Foegeding (2017).[2] This is a topic of high research activity in Latin American countries.[4,10,19,24,25]

In relation to the pharmaceutical industry, the use and interactions of insulin (INS) and chitosan (CS) have also been well reported in the literature.[7−10] INS is a peptide hormone produced by the pancreas that regulates glucose levels in the bloodstream. Type I diabetes arises when INS is not produced, and type II arises when production is scarce or the organism rejects it. In both cases (I and II) it is difficult for glucose to enter the cells, causing multiple adverse health effects.[11] INS is a therapeutically active protein and is used in the treatment of diabetes mellitus at the recommended dose of ≥0.4 U/kg.[12] Two polypeptide chains form INS: chain A consists of 21 amino acids, and chain B contains 30 amino acids. Chains A and B are held together by two disulfide (S−S) bridges. In addition, chain A also includes a third intrachain disulfide bridge, situated between residues 6 and 11.[13] On the other hand, CS is a biodegradable, biocompatible, and nontoxic polymer obtained from chitin. It is known that chitin is a byproduct that becomes an environmental pollutant derived from activities in fish farms. After a chemical modification, not only is the byproduct used but a new product with added value and new properties is obtained. The presence of $-NH_2$ and −OH groups gives to CS interesting chemical−biological properties.[14] The literature cites uses and properties for this polysaccharide as varied as enzyme immobilization, antimicrobial agent, in the preservation of food, promoter of plant growth, and absorption of metals and dyes, to name a few.[15]

As for INS and CS, these two versatile polymers allow the generation of a wide variety of complexes: it has been reported that bioadhesive chitosan-coated cationic nanoliposomes showed improved INS encapsulation and a prolonged oral hypoglycemic effect in diabetic mice.[16] Furthermore, CS−lecithin liposomal nanovesicles[17] have been tested as new carriers for oral delivery of INS, while Sadhasivam et al. have developed patches in order to evaluate the encapsulation efficiency and the release rate for transdermal delivery of INS.[18]

Moreover, INS−CS nanoparticle formation was explored by our group.[19] In this previous contribution a model that would explain the nanocomplex formation between human recombinant INS and a high molecular weight CS was proposed in order to be administrated through alternative ways than the parenteral, for instance oral or pulmonary.[20−22] However, one of the most interesting features of the nanocomplexes is their potential to trap and release the hormone they contain in a controlled manner. This release will depend, among other factors, on the pH, the temperature, or the ionic strength of the surrounding medium.[23] The INS and CS concentration conditions that allowed the formation of complexes were established and complexes with defined and reproducible submicronic dimensions were obtained. Complex formation was modulated by pH as the driving force involved in the process and the main type of chemical interactions between INS and CS were the electrostatic ones, established between specific titratable groups of each biopolymer: amine for CS and carboxylic for INS.

It is well-documented in the literature that the interplay between biocolloidal characteristics as size and charge, and extrinsic macromolecular properties as pH, ionic strength, and thermal energy results in a unique collection of mesoscopic forces for the molecular configuration and functionality in biological systems.[24,25] Different electrostatic coupling regimes can be observed depending on these physical chemical parameters. This work focus on the system constituted by INS and CS in a *weak* coupling regime, i.e. where *attraction* between both biopolymers can be experimentally seen and when they carry electric net charges of the same signal instead of the expected repulsive behavior as predicted by the classical DVLO theory.[26] This phenomenon can be described by Kirkwood's structure-sensitive electrostatic forces,[27] where mesoscopic *attractive* forces between macromolecules arise from fluctuations in titratable amino acid charges due to the induced shifts in the acid−base equilibrium. The attraction is pH-dependent and a result of an intrinsic physical property of the macromolecule, the capacitance (or the protein charge regulation parameter), which is a measure of the macromolecular net charge fluctuations (defined by the variance of the mean electrical charge) that is the determinant property for the "charge regulation mechanism".[28−30] The protein capacitance varies with solution pH as a consequence of the number of amino acid residues that titrate around each pH.[25] The attraction between charges alike has been called "complexation on the wrong side" of p*I* and reported in the literature for many other systems.[31,24,25,30,32]

The objective of this work was to investigate theoretically and to demonstrate via constant−pH Monte Carlo simulations that the complexation phenomenon (noncovalent linkages) between INS and the cationic polyelectrolyte CS is mainly driven by an electrostatic mechanism. The complexation process was modeled by a constant−pH scheme as it is well-known that pH can induce attraction between two titratable objects that results in stronger macromolecular association. The effect of the oligomeric states of INS was also investigated demonstrating that the number of INS molecules affects the complexation phenomena. CS self-association was assumed to be of minor importance to describe the main features of the INS−CS complexation and therefore is not explicitly included in the molecular model. The inclusion of a larger polymer chain or more chains would hamper the CPU time. Experimental results obtained from FTIR spectra and ζ-potential determinations allowed us to complement the conclusions.

2. MATERIALS AND METHODS

2.1. Materials. CS, MW = 300 kDa and deacetylation degree (DD) of 72%, was kindly donated by the Microbiology Laboratory of Instituto Nacional de Tecnología Industrial of Mar del Plata, Argentina. CS solutions were prepared with 1%, w/w, acetic acid.

Recombinant human INS was supplied by Denver Farma Laboratories, Buenos Aires, Argentina. The exact mass of INS was dissolved in 20 mM HCl solution, pH 2.

DOI: 10.1021/acs.jcim.9b00814
J. Chem. Inf. Model. XXXX, XXX, XXX−XXX

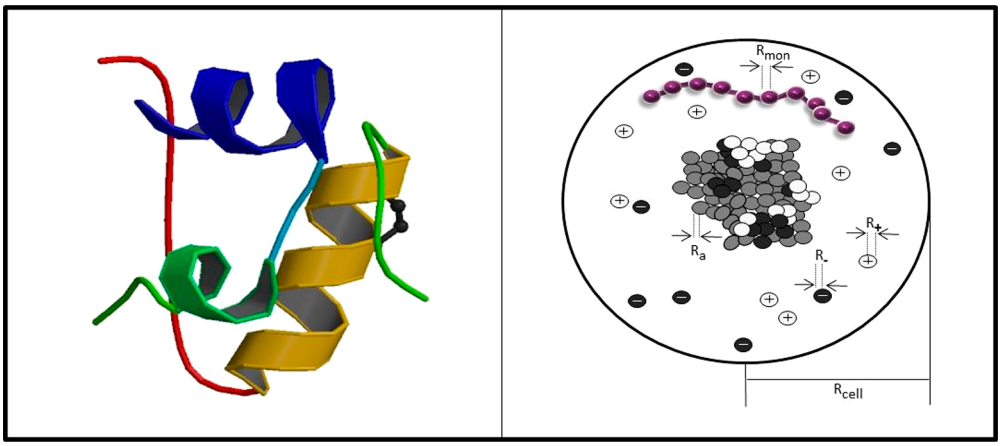

Figure 1. Macromolecular representations. (left) Structure of INS (chain A and B in the monomeric form at pH 6) as given by the crystallographic coordinates (PDB id 1APH). (right) Schematic representation of the INS−CS model system. INS is given in atomic details in a spherical electroneutral cell (radius R_{cell}) and is seen surrounded by counterions and added salt particles. Positive and negatively charged protein atoms (radii R_a) are represented in white and black, respectively. A flexible polyelectrolyte chain is used to model CS. The size of its monomers is R_{mon}.

All other chemicals were of analytical quality. Milli-Q water was always used. CS solutions were kept at 4 °C for 24 h to achieve the complete hydration of its molecules before its use.

2.2. Preparation of INS−CS complexes. For INS−CS nanoparticle preparation, each double concentrated biopolymer solution was mixed at pH 2, to give the required final concentrations of protein and polysaccharide in the bulk solution. INS solution was poured into CS solution under gently magnetic stirring and the mixed solution pH was increased up to 6 by careful addition of Na(OH), 4 N, solution, added drop by drop under stirring.

2.3. Optical Density Measurements. Each solution was freshly prepared and its optical density (OD) was registered upon time to study the formation of INS−CS complexes, at pH 2 and 6[33,34] using a PHERASTAR-FS microplate reader (BMG LabTech, Ortenberg, Germany). Optical density of INS solution was also registered as a control. Data was acquired at λ = 500 nm, away from INS and also CS intensity peaks.[35] Measurements were all performed at 25 °C; 200 μL of each solution was poured into each well with no additional preparation.

2.4. ζ-Potential Determinations. Briefly, INS and CS solutions were freshly prepared and their ζ-potential was measured for a pH range between 2 and 8. These measurements were carried out using a Zetasizer Nano-Zs particle analyzer (Malvern Instruments, Worcestershire, UK), as described by Silva et al.[19]

2.5. Freeze-Drying. INS and INS−CS solutions were lyophilized using a Stokes freeze-dryer operating at −40 °C condenser plate temperature and a chamber pressure of less than 100 μm Hg. After that they were dried in a vacuum oven at 40 °C in the presence of P_2O_5 to a constant weight.[36]

2.6. Infrared Spectroscopy. Fourier transform infrared (FTIR) spectra of lyophilized INS, CS, and INS−CS solutions were recorded on a Nicolet 8700 FT-IR Spectrometer with an ATR modulus. For each spectrum, a 64-scan interferogram was collected with 4 cm^{-1} resolution at room temperature. The data was processed with OMNIC 7.3 software from Thermo Electron Corporation. All samples were run in triplicate, and the results showed are the average of three measurements.

2.7. Theoretical Modeling. The molecular modeling began by considering the monomeric Human INS (chains A and B) in full atomistic details as a rigid body formed by a collection of charged hard spheres like beads. Each bead mimics a protein atom and is placed at the spatial coordinates given by the crystallographic structure available at the Protein Data Bank (PDB id 1APH) (Figure 1 left). This PDB file was edited before the calculations. All water molecules and heteroatoms were removed. The assigned radius for the INS beads (atoms) is 2.0 Å as suggested before in refs 37 and 32. Partial charges are assigned to beads depending on the physical chemical nature of the amino acids and as a function of the solution pH. Only specific atoms from titratable chemical groups [α-carboxyl, aspartyl carboxyl, glutamyl carboxyl, imidazole, α-amino, thiol (when not involved in SS bridges), phenolic, amino, and guanidyl] can be charged. All other atoms are assumed to be neutral. The protonation state of the ionizable groups can be altered during the simulations. This acid/base equilibrium is controlled by a protein titration scheme that considers any change in the environment including the pH, ionic strength, molecular concentration, presence of other charged objects (e.g., polysaccharide chain), and any variation of the protonation state of other titratable groups. This numerical scheme has been detailed described in previous works.[37,32,38] Different homo-oligomeric states were investigated. INS dimers, trimers, tetramers, and hexamers were built using the "GalaxyHomomer" server[39] with default parameters from the crystallographic structure (PDB id 1APH) in the monomeric form. This was necessary because our simulations did not include the self-aggregation process for INS. Since the focus of the work is on INS−CS complexation, we assumed that the INS homoassociation happened before its interaction with the polyelectrolyte chain. Therefore, an initial structure (dimer, tetramer, etc.) was chosen to be studied and calculations were repeated for all oligomeric states as there were done for the monomeric case.

For all oligomeric states, the protein INS as a monomer, dimer, trimer, tetramer, or hexamer was kept rigid, static, and in the same molecular configuration at the center of an electroneutral spherical cell with radius R_{cell} (Figure 1 right) determined by the protein concentration.[37] This corresponds to the so-called "cell model".[40]

Polyelectrolytes, such as CS, can be modeled as a flexible chain of charged monomers (beads) linked together with

DOI: 10.1021/acs.jcim.9b00814
J. Chem. Inf. Model. XXXX, XXX, XXX−XXX

harmonic springs. Following previous works,[37,32] we used a polycation chain with 21 beads with a radius (R_{mon}) of 2 Å. This is a reasonable number of monomers to describe the main physical interactions keeping a good balance between the real experimental conditions with the efficiency of the computational sampling. A larger chain would enhance the electrostatic interactions. At the same time, it would increase the CPU time. A uniform size of all beads was necessary to mimic the monomeric units of CS that also have the same size. Such chain is flexible and can freely move inside the cell, interacting with the protein atoms, counterions and added monovalent ions. Complementary simulations were also carried out with a polyanion in order to explore CS in both acid and basic regimes. Only one chain was included in the simulation cell. For the sake of simplicity, we have assumed that the charges of the monomers were fixed and fully protonated (a high degree of deacetylation) for all simulated pH conditions. This implies that the observed bimolecular interactions for solution pH $\gg$ 6.5 (the pK_a of the amino group in CS is ~6.5) tend to be overestimated. This should have a minor impact in our study since we are working on pH < 8, and most of the practical applications of CS are at the acid regime.[41]

Added salt and counterions were modeled by the usual restricted primitive model.[42] Each mobile ion k (added salt and counterions), with a q_k charge is considered as a charged hard sphere of radius R_a equals to 2.0 Å, while the solvent is effectively considered as a continuous dielectric medium without an explicit molecular structure and characterized by its relative static dielectric permittivity ε_s.

The combination of the cell model with the primitive one, the titration scheme and the modeling procedure for the polyelectrolyte chain defines the constant-pH coarse grained (CG) model, previously described by Barroso da Silva and coauthors[37,32,43,44,25] aiming to explore the protein complexation phenomena with the focus on electrostatic interactions and invoking a minimum set of parameters. The reader is referred to these cited papers[37,32,43,44,25] for more details about the model and the chosen parameters.

The interaction potential energy between any two particles i and j $[U^{ele}(r_{ij})]$ is given the combination of the Coulombic interaction with the hard-sphere model (eq 1):

$$U^{ele}(r_i) = \begin{cases} \dfrac{q_i q_j e^2}{4\pi\varepsilon_0\varepsilon_s r_{ij}}, & r_{ij} \le R_i + R_j \\ \infty, & \text{otherwise} \end{cases} \quad (1)$$

where ε_0 is the vacuum permittivity, q_i and q_j are the particles charge i (radius R_i) and j (radius R_j), respectively, and r_{ij} is their separation distance. This potential of interaction without a van der Waals attractive term guarantees that attraction is only possible via the electrostatic interactions.

The polyelectrolyte (polycation or polyanion) monomer−monomer interaction (βu^{bond}) was modeled by (eq 2)

$$\beta u^{bond} = \frac{l_b}{2r_{min}^3} \sum_{i=1}^{N_{mon}-1} (r_{i,i+1})^2 \quad (2)$$

where l_b is the Bjerrum length, $r_{i,i+1}$ is the separation between the consecutive monomers i and $i + 1$, r_{min} is the separation corresponding to the energy minimum for a dimer. As in previous studies, we have assumed r_{min} equals to 4 Å which results in an average monomer−monomer separation of approximately 7.4 Å.

All the mobile particles (polyelectrolyte beads, counterions, and added salt particles) are kept inside the simulation cell via an external potential $[U^{ext}(r_i)]$ (eq 3):

$$U^{ext}(r_i) = \begin{cases} 0, & r_i \le R_{cell} \\ \infty, & \text{otherwise} \end{cases} \quad (3)$$

The total energy of the system for a given configuration $[U(\{r_k\})]$ is given by the combination of eqs 1−3:

$$U(\{r_k\}) = \sum_{i=1}^{N_c+N_s} U^{ext}(r_i) + \frac{1}{2}\sum_{i=1}^{N}\sum_{j=1}^{N} U^{ele}(r_{ij}) + \beta u^{bond} \quad (4)$$

where N_c is the number of counterions, N_s is the number of added salt particles, and $N = N_c + N_s + N_P + N_{mon}$, which also includes the total number of charged protein atoms (N_P) and the number of polyelectrolyte monomers (N_{mon}). Note that the N_c is a different number when the polyelectrolyte is a polycation (CS for pH < 6.5) or a polyanion (CS for pH ≥ 6.5).

2.8. Simulation Details. The computer simulations were performed in a semigrand-canonical ensemble using the standard Metropolis Monte Carlo (MC) algorithm[45] with random translational displacements of mobile species (counterions, added salt particles, and polyelectrolyte monomers) within the electroneutral simulation cell and the titration movements.[37] A proton reservoir was set up within the cell to define a constant pH for the system. The solved constant-pH (CpH) CG model keeps constant the number of particles while the individual charges can vary during the simulation due to the protonation/deprotonation process.[32]

For each simulation, at least 10^9 MC steps were necessary for the system equilibration. They were followed by 10^{10} MC steps for production that were used for the measurements and analyses. R_{cell} was assumed to be equal to 150 Å which corresponds to a protein concentration of 58.7 mM. Salt concentration (NaCl) was fixed at 1.2 mM, while the solution pH was varied from 4 to 8. Temperature was 298 K, and therefore, ε_s was 78.7 in all simulation runs. At least three simulation replicas were carried out to confirm the convergence.

The main physical chemical quantity necessary for the present discussion is the free energy of interactions. Nevertheless, simulations with flexible chains in a solvent are well-known to be a special difficult case for free energy calculation due to the large energy barriers.[46] This problem can be solved by means of the penalty function protocol that we proposed in a previous work.[37] Alternatively, as it was recently demonstrated,[32,44] the sampling can also be sped up and the CPU time saved by means of the calculation and analysis of the product between the radial distribution function $[g(r)]$ and the square of the separation distance (r^2). Therefore, we followed this second protocol here to reduce the CPU time and be able to study larger oligomeric states. During the production runs, $g(r)$ was computed for the polymer beads−protein center based on histograms with 1 Å size. After the simulation, $g(r)$ were multiplied by r^2 and analyzed as done in refs 44 and 47.

DOI: 10.1021/acs.jcim.9b00814
J. Chem. Inf. Model. XXXX, XXX, XXX−XXX

3. RESULTS

3.1. pH Determinations. In order to experimentally determine the optimal pH that would maximize electrostatic interactions between hexameric INS and CS, ζ potential determinations were carried out. Such ζ potential values (mV) can be seen in Table 1. It is important to notice that initial pH conditions for INS correspond to the dimeric state for the protein,[48] but with increasing pH, the number of INS units also increases and corresponds to the hexameric conformation of the protein when the system reaches pH 6.

Table 1. ζ-Potential Values (mV) vs Solution pH for INS and CS Solutions[a]

pH	INS	CS
3	20.6 ± 2.1	5.8 ± 2.8
4	17.4 ± 1.3	6.8 ± 0.7
5	**−9.5 ± 0.7**	**6.5 ± 0.5**
6	**−32.4 ± 2.2**	**5.5 ± 0.7**
8	−39.1 ± 3.3	−17.9 ± 0.8
9	−44.6 ± 1.9	−20.5 ± 1.6

[a]Ionic strength I = 0.15 M. INS 0.2% w/v, CS 1 × 10^{-3}% w/v, at 25 °C. The number of INS units depends on the considered pH. Mean ± SD, n = 3.

For acidic pHs, lower than 5, both species (INS and CS) present positive net charges, therefore, attractiveness forces via electrostatic Coulombic interactions would be ruled out into the DVLO framework,[26] the interactions between like charged macroparticles are always repulsive due to the repulsive Coulombic contribution. In a similar manner, for alkaline pHs greater than 8, ζ-potential values are negative for both INS and CS, and electrostatic Coulombic repulsion is to be expected. In a pure Coulombic context, based on the ζ potentials, the INS−CS complexation could only be observed for the solution pH window between 5 and 6 (see the highlighted data in Table 1).

On the other hand, the experimentally determined ζ potential corresponding to mixed systems for 4.5 < pH < 6, hints that the probability of electrostatic interactions decreases, because the superficial charge of both macromolecules presents the same sign for this pH solution range.[19] A turbidity increases in mixed solutions, by naked-eye observation, also would indicate INS−CS interactions.

Such a phenomenon was not observed for single INS and CS solutions at this pH range. It is important to note that interactions of different physical natures than electrostatic, such as hydrophobic, van der Waals forces, etc., could be taking an important role, even though local electrostatic interactions between charged groups could not be completely discarded.

The INS molecule contains many ionizable groups, due to 6 amino acid residues capable of attaining a positive charge and 10 amino acid residues capable of attaining a negative charge. The net charge of the INS molecule as a function of pH solution calculated on the basis of amino acids intrinsic pK_a values was found by Tanford and Epstein.[49] The net charge is zero at pH 5.5, in good agreement with the electrophoretically determined isoelectric pH of 5.3−5.4.[50] These results are also in accordance with those obtained by a combination of modern techniques, as presented in the Open Chemistry Data Base, on the Pub Chem Web site (National Center for Biotechnology Information. PubChem Compound Database; CID = 16129672).[73]

Our results showed that under the following experimental conditions, 0.2% w/v, I = 0.15 M, 25 °C, INS presented a net zero charge at pH 5.0, as obtained by experimental ζ potential determination.[19] The discrepancy among the experimental and reported data, could obey to the different methodological techniques applied and other physical chemical parameters as the ionic strength, protein concentration or even a different protein genetic variant. For instance the pioneering work of Wintersteiner and Abramson in 1933[51] found a pI value for INS of 5.4 derived from turbidity measurements, which was in accordance with the result of the electrophoretic results from adsorbed or amorphous INS presented in the same contribution. The authors also found a pI value of 5.55 to 5.60 derived from the solubility based on measurements; which was considered less robust and susceptible to be discarded because the method of determination. Righetti and Caravaggio (1976) reported pIs for bovine and porcine INS, via isoelectric focusing, with values of 5.72 and 6, respectively.[52] As will be commented to a greater extent below, the theoretical predicted pI for INS obtained by the present constant-pH MC simulations is also within the interval 5.4−5.6 depending on the oligomeric state.

Taking into account the experimentally determined INS pI and considering that the CS pK_a is reported to be 6.5,[41] a solution pH of 6 was selected for the INS−CS nanocomplex generation. At this solution pH, the macromolecular attraction is expected to be maximum due to the net charges of INS and CS in a Coulombic framework.

3.2. Optical Density Measurements. INS aggregation kinetics were monitored by registering changes in optical density (OD) of INS−CS solutions over time, for solution pH 6 and ionic strength of 0.15 M. Turbidimetric studies applied to protein−polysaccharide systems are based on the fact that turbidity/OD is proportional to both size and concentration of the particles formed.[53] The experimental data was then fitted using the model proposed by Stirpe et al.,[54] a non-linear square curve-fitting to the following stretched exponential function (eq 5):

$$\mathrm{OD}(t) = \mathrm{OD} + \gamma \exp(-\alpha t)^{\beta} \quad (5)$$

where **OD**, **OD**$_0$, and $\boldsymbol{\gamma}$ are the observed optical density value at time t, the final optical density value, and the preexponential factor defined as optical density amplitude, respectively, whereas $\boldsymbol{\alpha}$ and $\boldsymbol{\beta}$ are the rate and the order of spontaneous aggregate formation.[54] Fitting data and the mathematical model applied corresponding to the kinetic parameters can be seen in Supporting Information. Values of $\boldsymbol{\alpha}$ and $\boldsymbol{\beta}$ derived from the fitting procedure in single INS and INS−CS complexes are reported in Table 2.

As it can be seen in Table 2, the INS−CS rate of protein aggregation almost triplicates the corresponding rate of single

Table 2. Kinetic Parameters That Describe the Protein Aggregation Process, from Experimental Data Fitting[a]

sample	α (1/min)	β
I	0.29 ± 0.01	2.2 ± 0.9
INS−CS	0.76 ± 0.16	2.1 ± 0.8

[a]Mean ± SD, n = 3. Ionic strength I = 0.15 M, INS 0.2% w/v, CS 1 × 10^{-4}% w/v.

DOI: 10.1021/acs.jcim.9b00814
J. Chem. Inf. Model. XXXX, XXX, XXX−XXX

INS. For single INS, the absence of solutes determines low rates of aggregation, behavior that notoriously changes with the presence of CS chains forming a dilute solution regime.[55]

The order of protein aggregates formation was similar for INS and INS−CS solutions, which could indicate that for this CS concentration, interactions between the protein and the polysaccharide chains were favored, i.e., both species were easily accessible due to, in part, the bridging flocculation phenomenon. Bridging-flocculation phenomenon is an analogy to the concept used in emulsion science. Briefly, the long polysaccharide chains are able to bind more than one protein aggregate, forming protein molecular clusters. Thus, each cluster is formed by charge neutralization and bridging effects. This effect is most pronounced at lower polysaccharide concentrations where protein aggregates surfaces are only partially covered. Under this phenomenon, long polysaccharide chains can bind protein aggregates and form molecular clusters due to charge neutralization and bridging effects; therefore not many intermediate steps were needed toward complexation.[56,57]

3.3. FT-IR Analysis. The interactions between INS and CS during the complexation process can be traced using infrared spectroscopy by comparing single INS and CS spectra with the spectrum obtained for the mixture (Figure 2). As can be seen, INS exhibits typical peaks around 1650 and 1540 cm^{-1}, that correspond to C═O stretching and C−N and N−H interactions, respectively.[58]

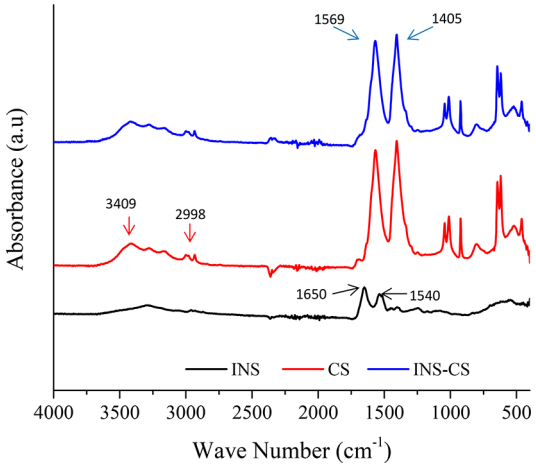

Figure 2. Infrared spectra of lyophilized INS, CS, and INS−CS complexes in the field 4000−500 cm^{-1}, at 25 °C and I = 0.15 M. Solutions were prepared at pH 6 prior to lyophilization.

On the other hand, the CS spectrum shows peaks around 3409 and 3283 cm^{-1} (O−H and N−H stretching), 2998 cm^{-1} (C−H stretch vibrations.), 1567 cm^{-1} (C═O tension in amide I), 1404 cm^{-1} (C−H and O−H deformation in amide II), 1013 cm^{-1} (C−O and C−H tension), and 808 cm^{-1} associated with the glucosamine units.[59−62]

In INS−CS complexes spectrum, single INS mean peaks (1650 and 1540 cm^{-1}) are masked. The characteristic absorption bands for the complexes appeared at 1569 and 1405 cm^{-1}. The first one could be assigned to a combination of signals from CS amide I and INS amide II. The second peak corresponds to CS; the small displacement from single CS spectrum could be associated with the interaction between the polymer and the protein at the level of amide II. No new peaks emergence was observed for the INS−CS complexes spectrum, which is in coincidence with the results obtained by Prusty and Sahu.[63] These observations suggest that some weaker physical interactions between INS and the polymer were formed during complexes formation, at least under these conditions of macromolecules concentration, pH, ionic strength, temperature, and solvent characteristics.

The findings presented in this contribution, regarding the effect upon complexation visualized through INS−CS FTIR spectra, are in line with those previously reported by Mukhopadhyay et al. and Sarmento et al.[58,64]

3.4. Numerical Simulations. In a pure DVLO approach the main physical driving force for the protein−polyelectrolyte complex formation is the Coulombic attraction, for oppositely charged particle systems. Conversely, for macromolecular species with like charges, the interaction would be always repulsive in this context. For macromolecules, however, the formation of soluble complexes can occur even when the protein and the polyelectrolyte present net charges with the same sign.[37,32,44] This has also been well reported in the literature in several experimental papers, for poly diallyldimethylammonium chloride (PDADMAC) and β-lactoglobulin,[65] for a cationic gold nanoparticle coupled to 3,6,9,12-tetraoxatricosan-1-aminium, 23-mercapto-*N*,*N*,*N*-trimethy (TTMA) and BSA[66] and several dendrimers and lysozyme,[67] just to cite a few examples.

As a result of a perturbation in the acid−base equilibrium, several changes can be induced in the distributions of charged groups, leading to the charge regulation mechanism enhancement.[44] These proton fluctuations evolve into an attractive mesoscopic electrostatic force, which in certain circumstances can overcome electrostatic Coulombic repulsion and allow complexes formation in the so-called "wrong side of p*I*".[68] This charge regulation phenomenon becomes particularly relevant under conditions, such as low ionic strength and pH close to the protein's p*I*.[37,32] It is at the p*I* that the repulsive Coulombic electrostatic interactions vanish, and the system should be dominated by the attractive interactions. However, depending on the magnitude of the main molecular characteristics (net charges and their charge regulation parameters) and the salt concentration, the attraction can be seen even further from the p*I*.

In order to comprehend the molecular mechanisms behind the INS−CS complexation mechanisms, simulations were performed at different pHs (the same pH range considered for experimental studies), while the number of INSs units was also varying. Along with a single chitosan chain, monomeric, dimeric, tetrameric, and hexameric INSs were considered [CS +nINS]. Thanks to these sets of simulations with different INS oligomeric states, it is possible to obtain the more adequate experimental conditions in terms of the solution pH and the number of INS units, which would favor complex formation. In this way a contrast between theoretical outcomes with the behavior given by the experimental techniques could be established. Additional CpH MC simulations runs were also performed with INS in the presence of an electrolyte solution as well as in the absence of CS. The purpose of this approach was to theoretically predict its isolated p*I* as a function of the oligomeric state. It was found that under these conditions, p*I* varies between 5.4 and 5.6. Monomers, dimers, and trimers have a p*I* equal to 5.4 while, for the tetramer, the p*I* increases to 5.5 and, for the hexamer, it is equal to 5.6.

DOI: 10.1021/acs.jcim.9b00814
J. Chem. Inf. Model. XXXX, XXX, XXX−XXX

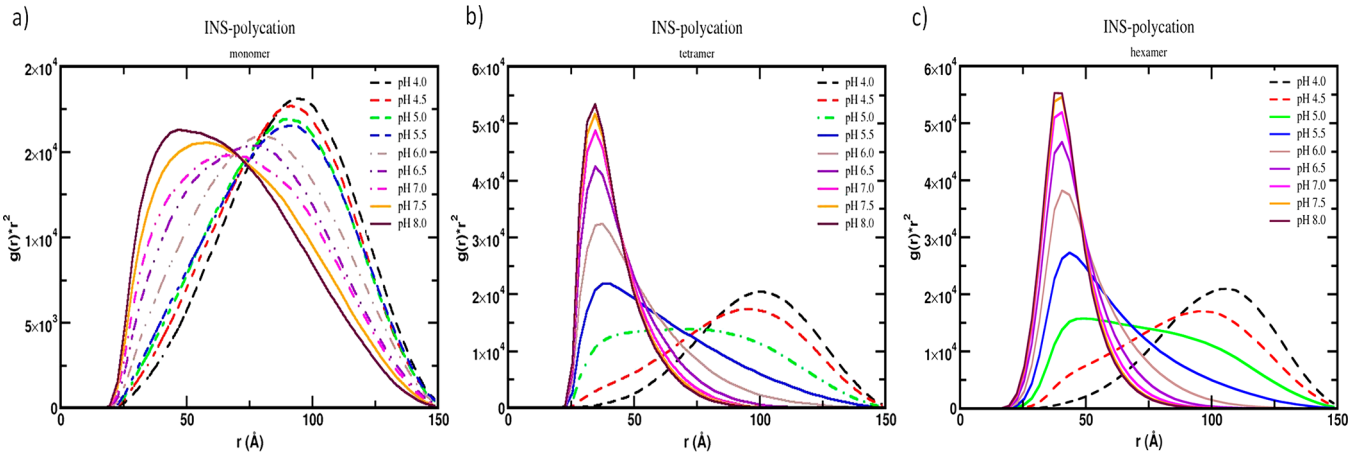

Figure 3. Computed free energy derivatives as a function of the separation distance between the protein center and the polyelectrolyte beads [$g(r)\cdot r^2$], for different numbers of INS units: (a) monomer; (b) tetramer; (c) hexamer. Different lines represent each complexation regime: solid (Coulombic attraction), dashed and dotted (attraction due the charge regulation mechanism), and dashed (Coulombic repulsion).

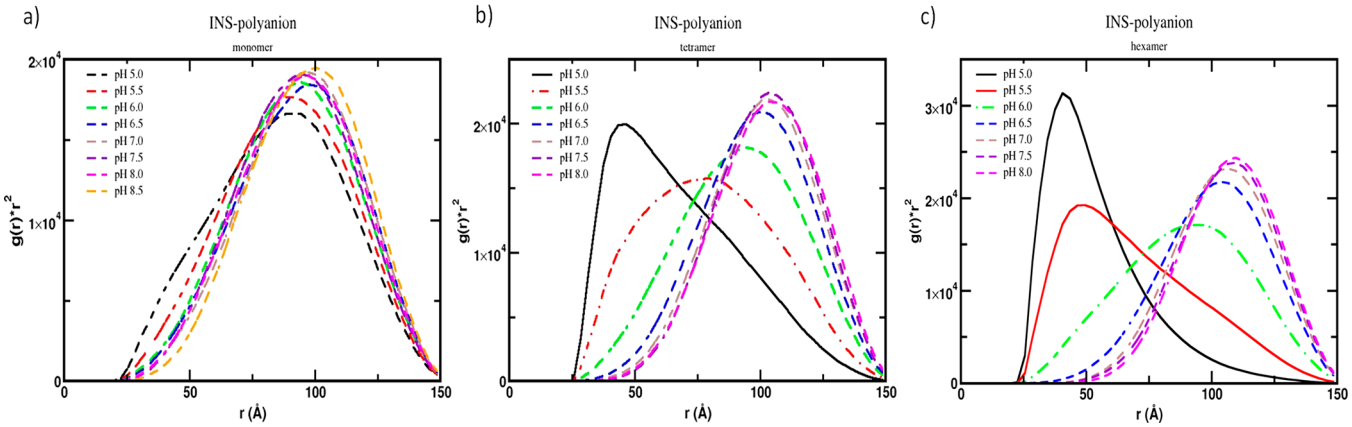

Figure 4. Computed free energy derivatives as a function of the separation distance between the protein center and the polyelectrolyte beads [$g(r)\cdot r^2$], for different numbers of INS units: (a) monomer; (b) tetramer; (c) hexamer. Different lines represent each regime: solid (Coulombic attraction), dashed and dotted (attraction due the charge regulation mechanism), and dashed (Coulombic repulsion).

These sets of simulations indicate that the interaction between INS and CS can follow the most common view of Coulombic interactions for some solutions pH values, where the complexation process requires for the macromolecules to have net charges with opposite sign. Besides these cases, complexation can also be observed for like-charged systems, as pointed out before. These cases with the complexation on the wrong side of p*I* are associated with the charge regulation mechanism.[37,32,44] For all the $g(r)\cdot r^2$ plots (see Figures 3−6), the highest the peak at the short separation distance regime, the stronger the attraction becomes. In a similar way, a high peak at a large distance indicates a significant repulsion. As regarding the lines, a solid one indicates complexation, a dotted−dash line suggests the complexation due to the charge regulation mechanism, and a dashed one represents a dominant repulsion mechanism in which no complexation process can be observed.

Before introducing the specific results from the different sets of simulations, it is relevant to highlight some experimental considerations from ζ potential measurements. This is also confirmed by the theoretical predicted titration data: for pH < 5.5, INS and CS present positive superficial charges, while for pH > 6.5 both charges are negative. The electrostatic Coulombic interaction pH has been established for 5.5 < pH < 6.5. Any attraction between these macromolecules observed for pH > 6.5, when both are negatively charged, would not have a Coulombic origin and could not be explained by the DVLO theory.

3.4.1. Polycation + nINS. Polycation + 1INS. This case corresponds to the system with a CS chain positively charged. In Figure 3, we present an estimative of the interaction free energy in terms of its derivative expressed by the product $g(r)\cdot r^2$. For the monomeric state of INS, a complexation INS−CS with low affinity can be spotted for alkaline pHs from 7.5 to 8, while a wider region where weaker attractions occurs can be seen for 6 < pH < 7. The two macromolecules are not firmly connected in these cases. The weaker attraction is probably due to the charge regulation mechanism that tries to overcome the Coulombic repulsion, not being strong enough to make it concrete. For more acidic pHs (pH ≤ 5.5), a repulsive interaction was obtained (see Figure 3a) following the classical Coulombic view where two positively charged macromolecules should repeal each other.

Polycation + 4INS. In Figure 3b, the effect of monomer number of INS units (aggregates) can be observed in terms of interaction. The change in the oligomeric state from the monomer to the tetramer results in stronger attraction in comparison with the monomeric case, previously exhibited in

DOI: 10.1021/acs.jcim.9b00814
J. Chem. Inf. Model. XXXX, XXX, XXX−XXX

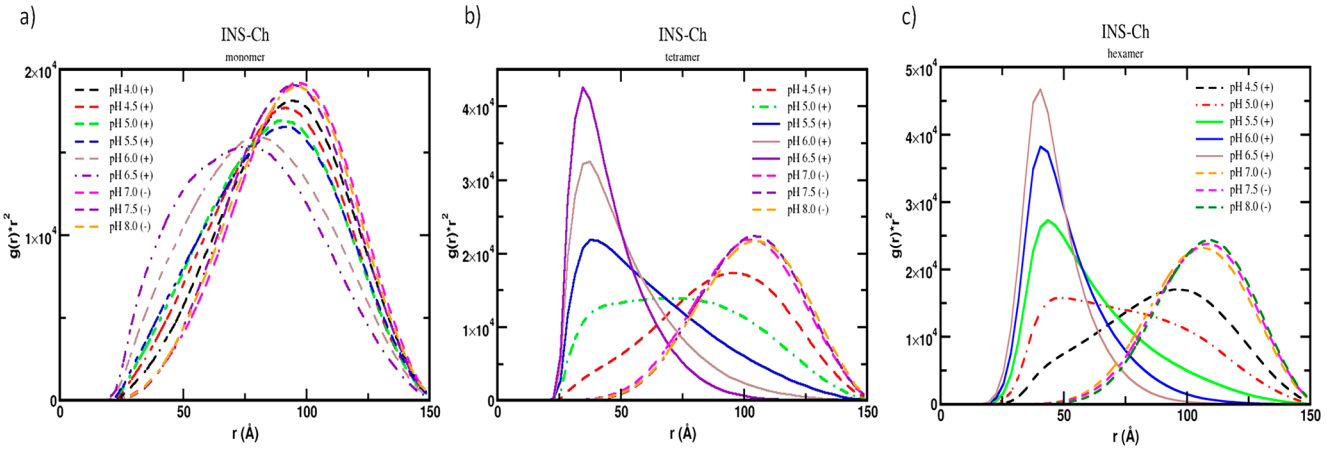

Figure 5. Computed free energy derivatives as a function of the separation distance between the protein center and the polyelectrolyte beads [$g(r)\cdot r^2$], for different numbers of INS units: (a) monomer; (b) tetramer; (c) hexamer. Different lines represent each regime: solid (Coulombic attraction), dashed and dotted (attraction due the charge regulation mechanism), and dashed (Coulombic repulsion).

Figure 3a. For the tetramer, complexation occurs for a pH range from 5.5 to 8, increasing its affinity as the solution pH value does (Figure 3b). 4INS (tetramer) is neutral at pH 5.5 which indicates that any attraction cannot be attributed to Coulombic interactions. The highest attraction for the 4INS case was detected at pH 8. On the other hand, pH 5 starts to be a condition where the attraction becomes weaker, and the interaction between the two macromolecules is weaker. The charge regulation mechanism manifests its effect but is not able to overcome the repulsive Coulombic interaction at pH 5. Under these conditions, no clear peak can be observed; hence, this case could be associated with a stage or phase prior to a real complexation, which could be associated with incipient complexation.

Polycation + 6INS. For INS on its hexameric form (Figure 3c), the complexation process continued the trend exhibited by 4INS (Figure 3b), with the exception that there was no evident charge regulation mechanism and the complexation directly starts at pH 5 and carried on until pH 8, where it showed a sharp intensity peak. For this set of simulations, an increase of INS units seemed to play a key role on the complexation process and in the characteristics of the complexes formed.

3.4.2. Polyanion + nINS. Polyanion + 1INS. We now turn to the case where the polyelectrolyte should mimic a CS negatively charged. An INS monomer and a polyanionic chain produced no complexation at all studied pH range, from 5 to 8.5, as it can be seen in Figure 4a. All the observed peaks presented separation distances of higher magnitude, which is characteristic of a repulsive interaction among the two macromolecules. It can be inferred from both experimental data and the predicted theoretical titration behavior of INS that, for a pH > 6.5, (i.e., CS's pK_a), INS and CS have the same negative sign being both species highly soluble. Therefore, electrostatic Coulombic interactions would not be favored for the complexation process to occur by this driving force.[25]

Polianion + 4INS. When the number of INS units increases (from 1INS to 4INS), the attraction increases again. Complexation occurred at pH 5, as can be observed in Figure 4b, while at pH 5.5 the trend seems to overcome the Coulombic repulsion with charge regulation mechanism. This result indicates that even when the Coulombic electrostatic interactions seem to be dominant in the system, the complexation process carries on due to the increase in the number of INS units. This particle association occurs for pHs in which both species have the same sign in terms of their net charges, or for pHs closer to the protein's p*I*s. This incipient interaction may arise from the fact that many of INS amino acids have isoelectric points between 5 and 6. For these interaction pHs, some precipitation can be experimentally observed at macroscopic scale, which is a signal of insoluble complex formation.

Polianion + 6INS. Incipient complexation was detected at pH 6. The complexation process due to Coulombic attraction occurs at pH 5 and 5.5, thus maintaining the tendency for 4INS and exhibiting complexation "on the wrong side of p*I*".

3.4.3. Chitosan + nINS. In Figure 5, we combined the data for the polycation and polyanion mimicking CS at both acid (+) and basic regimes (−). From this data, it can be concluded that complexation process is not expected for INS−CS when INS is in its monomeric form (Figure 5a). For both tetrameric and hexameric forms of INS (Figure 5b, c), incipient complexation due to charge regulation mechanism only took place at pH 5 and complexation range was observed to be 5.5 < pH < 6.5.

When the number of INS units increases in the simulation process, the solution pH at which the complexation can occur shifts toward acidic conditions. For example, while considering 3INS (not shown), this mechanism arises for 5.5 < pH < 6.5. Under these conditions, the highest intensity complexation occurs for pHs 6 and 6.5. Such behavior resembles the experimental conditions: for pH 5, where complexation and precipitation started, and at pH 6 where electrostatic interactions are maximized. While considering a protein aggregate of 4INS (p*I* = 5.5), complexation occurred for a range of pHs, 5.5 < pH < 6.5, with the highest intensity peaking at pH 6.5 even if both macromolecules have charges with the same sign. Charge regulation mechanism gives the weaker attraction for pH 5, as can be seen in Figure 5b. For pH < 4.5 and pH > 7, no attractive interactions were registered. Complexation for aggregates of 6INS (Figure 5c) resulted much more intense than for 4INS aggregates, even though on the same pH range, highlighting the importance of INS molecules number forming the aggregates to be associated with the polysaccharide.

From these sets of simulations, it can be presumed that INS−CS interactions certainly depend on the number of INS

DOI: 10.1021/acs.jcim.9b00814
J. Chem. Inf. Model. XXXX, XXX, XXX−XXX

units. In fact, in Figure 6, it can be observed not only how the complexation can be propitiated but also how this process also adds intensity for an increasing INS number in the oligomeric state.

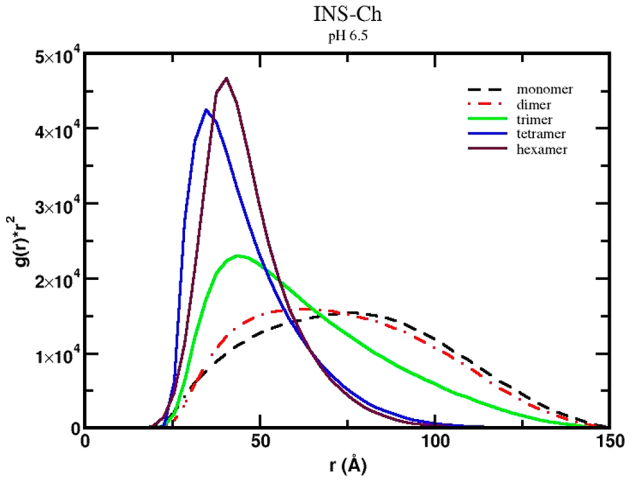

Figure 6. Computed free energy derivatives as a function of the separation distance between the protein center and the polyelectrolyte beads [$g(r)\cdot r2$], for different number of INS units at pH 6.5. Different lines represent each regime: solid (Coulombic attraction), dashed and dotted (attraction due the charge regulation mechanism), and dashed (Coulombic repulsion). The oligomeric state (from monomer to hexamer) is indicated in the plot.

It is important to highlight the fact that each simulation was conducted considering a fixed number of INS units, a condition maintained for the entire duration of the simulation procedure. Meanwhile, the experimental results showed that this number can vary as long as pH does.[53] For the simulations, is also important to note that when the number of INS monomers is changed during the process, the pH range at which the complexation occurs also changes, while the experimental data shows that the complexation process is favored at a fixed pH range.

Even more, it needs to be considered that both the protein and the polysaccharide used in this point, i.e. simulation approach, constitutes an oversimplification of a highly complex real situation, and therefore some differences may appear while comparing the simulated interaction pHs and those obtained from experimental data.[44] Nevertheless, this computational approach provides a practical mean to rationalize the complex interplay of the physical and chemical interactions involved in the process.

The set of figures presented here suggests that CS's chain interacts more efficiently, i.e. in a wider pH range, with INS aggregates formed by the highest monomer number; these results are in line with those experimentally obtained in ref 19. As a result of considering one polymeric chain interacting with one or several INS units, the comparison between simulations and experimental findings become difficult, because the experimental results indicate that multiple units of CS and INS as well, are involved in the complete complexation process. Furthermore, it has been described that both species have pH dependent self-aggregation kinetics that cannot be discarded,[69−71] even though the concentrations used in this work were low enough to minimize this effect.[72]

4. CONCLUSIONS

Experimental techniques proved the existence of macromolecular interactions between INS and CS, allowing us to obtain quantitative parameters that characterize the complexation process. Protein aggregation induced by the CS presence was monitored by turbidimetric measurements and during complexes formation. All the techniques combined allowed us to determine that pH 6 was the more appropriate level for maximizing complex formation via electrostatic interactions.

The chemical groups involved in such interactions were highlighted by FTIR, in dehydrated systems for which the complexation had already occurred in aqueous solution. Interactions between INS and CS were manifested by the subtle displacement of peaks corresponding to amide I and amide II in the formed complex.

Modeling data derived from the turbidimetric measurements allowed to establish that, under a dilute regime, complexation phenomenon proceeds rapidly, and the type of structure formed is a cluster formed via bridging flocculation.

On the other hand, constant-pH Monte Carlo simulations were performed in order to further elucidated INS−CS interactions and complex formation. These simulations showed that two parameters are the most relevant for the INS−CS complexation process. On one hand, as the INS unit number increases so does the complexation probability. On the other hand, the pH should be higher than 5.5 for macromolecular interactions, which correlates with ζ-potential measurements, indicating that the experimental pH range should be 5.5 < pH < 6.5. This ζ-potential range ensures the electrostatic interactions between the two species.

In this context, the charge regulation mechanism can be considered as a previous phase toward complexation or an incipient complexation stage caused by weak interactions of Coulombic nature. In any case, this mechanism should not be ruled out, especially for pHs that render both species with the same net charges or at pH values that are too close with protein p*I*. Simulations turned out to be a very interesting tool to elucidate a pH-induced mechanism that could translate into attractive forces due to electrostatic interactions and repulsive forces for situations in which the macromolecules have the same surface charge.

These results are of extreme relevance, because pH, and therefore the INS aggregation state or the number of aggregated monomers (*n*INS), must be carefully considered for a complete process understanding. In this context these results are in line with those published before in the work of Silva et al.[19]

From a technological point of view, the knowledge of INS−CS parameters that rule complex formation could be an alternative for developing a new generation of drugs allowing INS protection from the hostile conditions of the body and increasing its absorption. In summary, these findings have basic and practical impacts as they could be exploited to exert the controlled release of INS in therapeutic formulations by using CS based complexes.

■ ASSOCIATED CONTENT

Supporting Information

The Supporting Information is available free of charge at https://pubs.acs.org/doi/10.1021/acs.jcim.9b00814.

Table S1 and Figure S1 (PDF)

DOI: 10.1021/acs.jcim.9b00814
J. Chem. Inf. Model. XXXX, XXX, XXX−XXX

AUTHOR INFORMATION

Corresponding Author

*Email: flbarroso@usp.br.

ORCID

Cecilia Prudkin-Silva: 0000-0001-8593-845X

Oscar E. Pérez: 0000-0002-8223-1077

Karina D. Martínez: 0000-0002-5208-6067

Fernando L. Barroso da Silva: 0000-0003-2526-2085

Notes

The authors declare no competing financial interest.

ACKNOWLEDGMENTS

C.P.S., O.E.P., and K.D.M. thank Universidad de Buenos Aires [Project 20020150100079BA]; Agencia Nacional de Promoción Científica y Tecnológica (ANPCyT) [(PICT 2015-3866 and PICT2017-1683); and CONICET of Argentina for support. F.L.B. thanks the Fundação de Amparo à Pesquisa do Estado de São Paulo [Fapesp 2015/16116-3], the Conselho Nacional de Desenvolvimento Cientifico e Tecnológico (CNPq), and the USP through the NAP-CatSinQ (Research Core in Catalysis and Chemical Synthesis) for support and Rice University for computing hours through the international collaboration program with USP and at The Swedish National Infrastructure for Computing (SNIC 2019/1-32) where part of the simulations were performed.

REFERENCES

(1) Kocak, G.; Tuncer, C.; Bütün, V. PH-Responsive Polymers. *Polym. Chem.* **2017**, *8* (1), 144−176.

(2) Wagoner, T. B.; Foegeding, E. A. Whey Protein−Pectin Soluble Complexes for Beverage Applications. *Food Hydrocolloids* **2017**, *63*, 130−138.

(3) Feng, Z.; Zhang, T.; Wang, H.; Xu, B. Supramolecular Catalysis and Dynamic Assemblies for Medicine. *Chem. Soc. Rev.* **2017**, *46* (21), 6470−6479.

(4) Mendes, A. C.; Baran, E. T.; Reis, R. L.; Azevedo, H. S. Self-Assembly in Nature: Using the Principles of Nature to Create Complex Nanobiomaterials. *Wiley Interdiscip. Rev. Nanomedicine Nanobiotechnology* **2013**, *5* (6), 582−612.

(5) Smirnova, E.; Safenkova, I.; Stein-Margolina, V.; Shubin, V.; Polshakov, V.; Gurvits, B. PH-Responsive Modulation of Insulin Aggregation and Structural Transformation of the Aggregates. *Biochimie* **2015**, *109* (December), 49−59.

(6) Palao-Suay, R.; Gómez-Mascaraque, L. G.; Aguilar, M. R.; Vázquez-Lasa, B.; Román, J. S. Self-Assembling Polymer Systems for Advanced Treatment of Cancer and Inflammation. *Prog. Polym. Sci.* **2016**, *53*, 207−248.

(7) Fernández-Urrusuno, R.; Calvo, P.; Remuñán-López, C. Enhancement of Nasal Absorption of Insulin Using Chitosan Nanoparticles. *Pharm. Res.* **1999**, *16* (10), 1576.

(8) Ma, Z.; Yeoh, H. H.; Lim, L. Y. Formulation PH Modulates the Interaction of Insulin with Chitosan Nanoparticles. *J. Pharm. Sci.* **2002**, *91* (6), 1396−1404.

(9) He, Z.; Santos, J. L.; Tian, H.; Huang, H.; Hu, Y.; Liu, L.; Leong, K. W.; Chen, Y.; Mao, H. Q. Scalable Fabrication of Size-Controlled Chitosan Nanoparticles for Oral Delivery of Insulin. *Biomaterials* **2017**, *130*, 28−41.

(10) Gatti, T. H. H.; Eloy, J. O.; Ferreira, L. M. B.; Da Silva, I. C.; Pavan, F. R.; Gremião, M. P. D.; Chorilli, M. Insulin-Loaded Polymeric Mucoadhesive Nanoparticles: Development, Characterization and Cytotoxicity Evaluation. *Brazilian J. Pharm. Sci.* **2018**, *54* (1), 1−10.

(11) Roglic, G.; Norris, S. L. Guidelines on Second-and Third-Line Medicines and Type of Insulin for the Control of Blood Glucose Levels in Non-Pregnant Adults with Diabetes Mellitus. *Ann. Intern. Med.* **2018**, *169*, 394−397.

(12) Naha, P.; Kanchan, V.; Manna, P. K.; Panda, A. K. Improved Bioavailability of Orally Delivered Insulin Using Eudragit-L30D Coated PLGA Microparticles. *J. Microencapsulation* **2008**, *25* (4), 248−256.

(13) Sharma, S.; Jyoti, K.; Sinha, R.; Katyal, A.; Jain, U. K.; Madan, J. *Protamine Coated Proliposomes of Recombinant Human Insulin Encased in Eudragit S100 Coated Capsule Offered Improved Peptide Delivery and Permeation across Caco-2 Cells*; Elsevier B.V., 2016; Vol. *67*.

(14) Shukla, S. K.; Mishra, A. K.; Arotiba, O. A.; Mamba, B. B. Chitosan-Based Nanomaterials: A State-of-the-Art Review. *Int. J. Biol. Macromol.* **2013**, *59*, 46−58.

(15) Kaur, S.; Dhillon, G. S. The Versatile Biopolymer Chitosan: Potential Sources, Evaluation of Extraction Methods and Applications. *Crit. Rev. Microbiol.* **2014**, *40* (2), 155−175.

(16) Shalaby, T. I.; El-Refaie, W. M. *Bioadhesive Chitosan-Coated Cationic Nanoliposomes With Improved Insulin Encapsulation and Prolonged Oral Hypoglycemic Effect in Diabetic Mice*; American Pharmacists Association, 2018; Vol. *107*.

(17) Al-Remawi, M.; Elsayed, A.; Maghrabi, I.; Hamaidi, M.; Jaber, N. Chitosan/Lecithin Liposomal Nanovesicles as an Oral Insulin Delivery System. *Pharm. Dev. Technol.* **2017**, *22* (3), 390−398.

(18) Sadhasivam, L.; Dey, N.; Francis, A. P.; Devasena, T. Transdermal Patches of Chitosan Nanoparticles for Insulin Delivery. *Int. J. Pharm. Pharm. Sci.* **2015**, *7* (5), 84−88.

(19) Silva, C. P.; Martinez, J. H.; Martinez, K. D.; Farias, M. E.; Leskow, F. C.; Perez, O. E. Proposed Molecular Model for Electrostatic Interactions between Insulin and Chitosan. Nano-Complexation and Activity in Cultured Cells. *Colloids Surf., A* **2018**, *537*, 425−434.

(20) Gaul, R.; Ramsey, J. M.; Heise, A.; Cryan, S.-A.; Greene, C. M. *Nanotechnology Approaches to Pulmonary Drug Delivery: Targeted Delivery of Small Molecule and Gene-Based Therapeutics to the Lung*; Elsevier Inc., 2018.

(21) Gedawy, A.; Martinez, J.; Al-Salami, H.; Dass, C. R. Oral Insulin Delivery: Existing Barriers and Current Counter-Strategies. *J. Pharm. Pharmacol.* **2018**, *70* (2), 197−213.

(22) Khafagy, E. S.; Morishita, M.; Onuki, Y.; Takayama, K. Current Challenges in Non-Invasive Insulin Delivery Systems: A Comparative Review. *Adv. Drug Delivery Rev.* **2007**, *59* (15), 1521−1546.

(23) Ichikawa, S.; Iwamoto, S.; Watanabe, J. Formation of Biocompatible Nanoparticles by Self-Assembly of Enzymatic Hydrolysates of Chitosan and Carboxymethyl Cellulose. *Biosci., Biotechnol., Biochem.* **2005**, *69* (9), 1637−1642.

(24) Jönsson, B.; Lund, M.; Barroso Da Silva, F. L. Electrostatics in Macro-Molecular Solutions. In *Food Colloids: Self-Assembly and Material Science*; Dickinson, E., Leser, M. E., Eds.; Royal Society of Chemistry: Cambridge, 2007; p 129.

(25) da Silva, F. L. B.; Jonsson, B. Polyelectrolyte−Protein Complexation Driven by Charge Regulation. *Soft Matter* **2009**, *5* (15), 2862.

(26) Verwey, E. J. W.; Overbeek, J. T. G.; Overbeek, J. T. G. *Theory of the Stability of Lyophobic Colloids*; Courier Corporation, 1999.

(27) Kirkwood, J. G.; Shumaker, J. B. Forces between Protein Molecules in Solution Arising from Fluctuations in Proton Charge and Configuration. *Proc. Natl. Acad. Sci. U. S. A.* **1952**, *38* (10), 863−871.

(28) De Vos, W. M.; Biesheuvel, P. M.; De Keizer, A.; Kleijn, J. M.; Stuart, M. A. C. Adsorption of the Protein Bovine Serum Albumin in a Planar Poly(Acrylic Acid) Brush Layer as Measured by Optical Reflectometry. *Langmuir* **2008**, *24* (13), 6575−6584.

(29) Lund, M.; Jönsson, B. Charge Regulation in Biomolecular Solution. *Q. Rev. Biophys.* **2013**, *46* (3), 265−281.

(30) Barroso Da Silva, F. L.; Boström, M.; Persson, C. Effect of Charge Regulation and Ion-Dipole Interactions on the Selectivity of Protein-Nanoparticle Binding. *Langmuir* **2014**, *30* (14), 4078−4083.

DOI: 10.1021/acs.jcim.9b00814
J. Chem. Inf. Model. XXXX, XXX, XXX−XXX

(31) De Kruif, C. G.; Weinbreck, F.; De Vries, R. Complex Coacervation of Proteins and Anionic Polysaccharides. *Curr. Opin. Colloid Interface Sci.* **2004**, *9* (5), 340−349.
(32) Srivastava, D.; Santiso, E.; Gubbins, K.; Barroso Da Silva, F. L. Computationally Mapping PKaShifts Due to the Presence of a Polyelectrolyte Chain around Whey Proteins. *Langmuir* **2017**, *33* (42), 11417−11428.
(33) Li, J.; Wu, Y.; Zhao, L. Antibacterial Activity and Mechanism of Chitosan with Ultra High Molecular Weight. *Carbohydr. Polym.* **2016**, *148*, 200−205.
(34) Tang, D. W.; Yu, S. H.; Ho, Y. C.; Huang, B. Q.; Tsai, G. J.; Hsieh, H. Y.; Sung, H. W.; Mi, F. L. Characterization of Tea Catechins-Loaded Nanoparticles Prepared from Chitosan and an Edible Polypeptide. *Food Hydrocolloids* **2013**, *30* (1), 33−41.
(35) Weijers, M.; Van De Velde, F.; Stijnman, A.; Van De Pijpekamp, A.; Visschers, R. W. Structure and Rheological Properties of Acid-Induced Egg White Protein Gels. *Food Hydrocolloids* **2006**, *20* (2−3), 146−159.
(36) Perez, O.; Haros, M.; Suarez, C. Corn Steeping: Influence of Time and Lactic Acid on Isolation and Thermal Properties of Starch. *J. Food Eng.* **2001**, *48* (10), 251−256.
(37) Barroso da Silva, F. L.; Lund, M.; Jönsson, B.; Åkesson, T. On the Complexation of Proteins and Polyelectrolytes. *J. Phys. Chem. B* **2006**, *110* (9), 4459−4464.
(38) Barroso da Silva, F. L.; Dias, L. G. Development of Constant-PH Simulation Methods in Implicit Solvent and Applications in Biomolecular Systems. *Biophys. Rev.* **2017**, *9* (5), 699−728.
(39) Baek, M.; Park, T.; Heo, L.; Park, C.; Seok, C. Galaxy Homomer: A Web Server for Protein Homo-Oligomer Structure Prediction from a Monomer Sequence or Structure. *Nucleic Acids Res.* **2017**, *45* (W1), W320−W324.
(40) Jönsson, B.; Wennerstrom, H. Thermodynamics of Ionic Amphiphile-Water Systems. *J. Colloid Interface Sci.* **1981**, *80* (2), 482−496.
(41) Olatunji, O. *Natural Polymers: Industry Techniques and Applications*; Springer International Publishing: Switzerland, 2016.
(42) Levesque, D.; Weis, J.; Hansen, J. *Monte Carlo Methods in Statistical Physics*; Binder, K., Ed.; Springer-Verlag: Berlin, 1986.
(43) Barroso Da Silva, F. L. *Peculiaridades Nos Mecanismos Moleculares de Proteinas Em Solução Aquosa: Exemplo Da Importância Do Equilíbrio Ácido-Base Para Aplicações Em Biotecnologia*; 2013; Vol. *131*.
(44) Montellano Duran, N.; Spelzini, D.; Wayllace, N.; Boeris, V.; Barroso da Silva, F. L. A Combined Experimental and Molecular Simulation Study of Factors Influencing Interaction of Quinoa Proteins−Carrageenan. *Int. J. Biol. Macromol.* **2018**, *107*, 949−956.
(45) Frenkel, D.; Smit, B. *Understanding Molecular Simulation: From Algorithms to Applications*; Academic Press: San Diego, 1996.
(46) Engkvist, O.; Karlström, G. A Method to Calculate the Probability Distribution for Systems with Large Energy Barriers. *Chem. Phys.* **1996**, *213* (1−3), 63−76.
(47) Montellano Duran, N. Propiedades Estructurales Y Funcionales de Las Proteínas de Chenopodium Quinoa y Sus Hidrolizados. *Univ. Nac. Rosario* **2017**, 1−11.
(48) Whittingham, J. L.; Scott, D. J.; Chance, K.; Wilson, A.; Finch, J.; Brange, J.; Dodson, G. G. Insulin at PH 2: Structural Analysis of the Conditions Promoting Insulin Fibre Formation. *J. Mol. Biol.* **2002**, *318* (02), 479−490.
(49) Tanford, C.; Epstein, J. The Physical Chemistry of Insulin. I. Hydrogen Ion Titration Curve of Zinc-Free Insulin. *J. Am. Chem. Soc.* **1954**, *76* (8), 2163−2169.
(50) Porath, J.; Hao Li, C. Elution and Displacement Analysis of Insulin and Adrenocorticotropic Peptides on Pre-Treated Carbon. *Biochim. Biophys. Acta* **1954**, *13*, 268−277.
(51) Wintersteiner, O.; Abramson, H. The Isoelectric Point of Insulin. Electrical Properties of Adsorbed and Crystalline Insulin. *J. Biol. Chem.* **1933**, *99* (3), 741−753.
(52) Righetti, P. G.; Caravaggio, T. Isoelectric Points and Molecular Weights of Proteins: A Table. *J. Chromatogr. A* **1976**, *127* (1), 1−28.
(53) Dunn, M. F. Zinc−Ligand Interactions Modulate Assembly and Stability of the Insulin Hexamer−a Review. *BioMetals* **2005**, *18*, 295−303.
(54) Stirpe, A.; Pantusa, M.; Rizzuti, B.; Sportelli, L.; Bartucci, R.; Guzzi, R. Early Stage Aggregation of Human Serum Albumin in the Presence of Metal Ions. *Int. J. Biol. Macromol.* **2011**, *49* (3), 337−342.
(55) Holthauzen, L. M. F.; Auton, M.; Sinev, M.; Rösgen, J. Protein Stability in the Presence of Cosolutes. *Methods Enzymol.* **2011**, *492*, 61.
(56) Juarez, J.; Lopez, S. G.; Cambon, A.; Taboada, P.; Mosquera, V. Influence of Electrostatic Interactions on the Fibrillation Process of Human Serum Albumin. *J. Phys. Chem. B* **2009**, *113* (30), 10521−10529.
(57) Matalanis, A.; Jones, O. G.; McClements, D. J. Structured Biopolymer-Based Delivery Systems for Encapsulation, Protection, and Release of Lipophilic Compounds. *Food Hydrocolloids* **2011**, *25* (8), 1865−1880.
(58) Mukhopadhyay, P.; Sarkar, K.; Chakraborty, M.; Bhattacharya, S.; Mishra, R.; Kundu, P. P. Oral Insulin Delivery by Self-Assembled Chitosan Nanoparticles: In Vitro and in Vivo Studies in Diabetic Animal Model. *Mater. Sci. Eng., C* **2013**, *33* (1), 376−382.
(59) Guo, L.; Liu, G.; Hong, R. Y.; Li, H. Z. Preparation and Characterization of Chitosan Poly(Acrylic Acid) Magnetic Microspheres. *Mar. Drugs* **2010**, *8* (7), 2212−2222.
(60) Alhosseini, S. N.; Moztarzadeh, F.; Mozafari, M.; Asgari, S.; Dodel, M.; Samadikuchaksaraei, A.; Kargozar, S.; Jalali, N. Synthesis and Characterization of Electrospun Polyvinyl Alcohol Nanofibrous Scaffolds Modified by Blending with Chitosan for Neural Tissue Engineering. *Int. J. Nanomed.* **2012**, *7*, 25−34.
(61) Venkatesham, M.; Ayodhya, D.; Madhusudhan, A.; Veera Babu, N.; Veerabhadram, G. A Novel Green One-Step Synthesis of Silver Nanoparticles Using Chitosan: Catalytic Activity and Antimicrobial Studies. *Appl. Nanosci.* **2014**, *4* (1), 113−119.
(62) Heuser, M.; Cárdenas, G. Chitosan-Copper Paint Types as Antifouling. *J. Chil. Chem. Soc.* **2014**, *59* (2), 2415−2419.
(63) Prusty, A. K.; Sahu, S. K. Development and Evaluation of Insulin Incorporated Nanoparticles for Oral Administration. *ISRN Nanotechnol.* **2013**, *2013*, 1−6.
(64) Sarmento, B.; Ferreira, D.; Veiga, F.; Ribeiro, A. Characterization of Insulin-Loaded Alginate Nanoparticles Produced by Ionotropic Pre-Gelation through DSC and FTIR Studies. *Carbohydr. Polym.* **2006**, *66* (1), 1−7.
(65) Xu, Y.; Mazzawi, M.; Chen, K.; Sun, L.; Dubin, P. L. Protein Purification by Polyelectrolyte Coacervation: Influence of Protein Charge Anisotropy on Selectivity. *Biomacromolecules* **2011**, *12* (5), 1512−1522.
(66) Chen, K.; Xu, Y.; Rana, S.; Miranda, O. R.; Dubin, P. L.; Rotello, V. M.; Sun, L.; Guo, X. Electrostatic Selectivity in Protein-Nanoparticle Interactions. *Biomacromolecules* **2011**, *12* (7), 2552−2561.
(67) Xu, X.; Angioletti-Uberti, S.; Lu, Y.; Dzubiella, J.; Ballauff, M. Interaction of Proteins with Polyelectrolytes: A Comparison between Theory and Experiment. *Langmuir* **2019**, *35*, 5373.
(68) Wang, X.; Zheng, K.; Si, Y.; Guo, X.; Xu, Y. Protein−Polyelectrolyte Interaction: Thermodynamic Analysis Based on the Titration Method. *Polymers (Basel, Switz.)* **2019**, *11*, 82.
(69) Huang, Y.; Lapitsky, Y. On the Kinetics of Chitosan/Tripolyphosphate Micro- and Nanogel Aggregation and Their Effects on Particle Polydispersity. *J. Colloid Interface Sci.* **2017**, *486*, 27−37.
(70) Baram, M.; Gilead, S.; Gazit, E.; Miller, Y. Mechanistic Perspective and Functional Activity of Insulin in Amylin Aggregation. *Chem. Sci.* **2018**, *9* (18), 4244−4252.
(71) Chung, L. H. C.; Birch, D. J. S.; Vyshemirsky, V.; Ryadnov, M. G.; Rolinski, O. J. Insulin Aggregation Tracked by Its Intrinsic TRES. *Appl. Phys. Lett.* **2017**, *111* (26), 263701.
(72) Philippova, O. E.; Volkov, E. V.; Sitnikova, N. L.; Khokhlov, A. R.; Desbrieres, J.; Rinaudo, M. Two Types of Hydrophobic Aggregates in Aqueous Solutions of Chitosan and Its Hydrophobic Derivative. *Biomacromolecules* **2001**, *2* (2), 483−490.

DOI: 10.1021/acs.jcim.9b00814
J. Chem. Inf. Model. XXXX, XXX, XXX−XXX

(73) https://pubchem.ncbi.nlm.nih.gov/compound/16129672 (accessed Dec 13, 2018).

DOI: 10.1021/acs.jcim.9b00814
J. Chem. Inf. Model. XXXX, XXX, XXX−XXX